Crew Exploration Vehicle Launch Abort Controller Performance Analysis

Dean W. Sparks, Jr.[*] and David L. Raney[†]
NASA Langley Research Center, Hampton, VA, 23681-2199

This paper covers the simulation and evaluation of a controller design for the Crew Module (CM) Launch Abort System (LAS), to measure its ability to meet the abort performance requirements. The controller used in this study is a hybrid design, including features developed by the Government and the Contractor. Testing is done using two separate 6-degree-of-freedom (DOF) computer simulation implementations of the LAS/CM throughout the ascent trajectory: 1) executing a series of abort simulations along a nominal trajectory for the nominal LAS/CM system; and 2) using a series of Monte Carlo runs with perturbed initial flight conditions and perturbed system parameters. The performance of the controller is evaluated against a set of criteria, which is based upon the current functional requirements of the LAS. Preliminary analysis indicates that the performance of the present controller meets (with the exception of a few cases) the evaluation criteria mentioned above.

Nomenclature

Acronyms

ACM = attitude control motor
AGL = above ground level
ANTARES = Advanced NASA Technology Architecture for Exploration Studies
CEV = Crew Exploration Vehicle
CLV = Crew Launch Vehicle
CM = Crew Module
ConOps = Concept of Operations
GRAM = Global Reference Atmospheric Model
KSC = Kennedy Space Center
LAS = Launch Abort System
LAV = Launch Abort Vehicle
LES = Launch Escape System
RCS = Reaction Control System
SM = Service Module

Symbols

α = angle-of-attack, °
α_{re} = set of angle-of-attack values in 1.5 sec interval prior to reorientation completion, °
α_{lim} = maximum acceptable angle-of-attack value prior to reorientation start, º
α_{total} = total angle-of-attack, º , with $\cos(\alpha_{total}) = \cos(\alpha)\cos(\beta)$
β = sideslip angle, º
dpr = dot product range, ft.
h = geodetic altitude, ft.
M = Mach number
p = body roll rate, º/sec.
q = body pitch rate, º/sec.
$\bar{q}$ = dynamic pressure, psf

[*] Aerospace Technologist, Dynamic Systems and Control Branch, Mail Stop 308.
[†] Aerospace Technologist, Dynamic Systems and Control Branch, Mail Stop 308, AIAA Member.

$\bar{q}_{can}$ = dynamic pressure while canards deployed, psf
r = body yaw rate, º/sec.

I. Launch Abort System Description

THE Launch Abort System (LAS) is required to provide a launch abort capability from the pad after Crew Module (CM) hatch closure throughout the Crew Launch Vehicle (CLV) ascent until orbital insertion. Figure 1 is an illustration of the Launch Abort Vehicle (LAV), which consists of the LAS and CM components of the Crew Exploration Vehicle (CEV). The third major component of the CEV is the Service Module (SM), however, aborts involving the SM are not included in this paper. The Apollo Launch Escape System (LES) relied on a passive approach that involved the use of open-loop timers to control the abort event sequencing, along with a passive aerodynamic canard that was deployed to reorient the vehicle to a heat-shield forward attitude following the escape motor firing and a brief coast period. While the Apollo LES had the virtues of lower risk and simplicity, there were drawbacks. The passive Apollo system required approximately 1,000 lb of ballast to ensure aerodynamic stability during the escape motor firing and coast, and the passive canard system could produce tumbling in some portions of the abort envelope before settling into a heat-shield forward attitude[1].

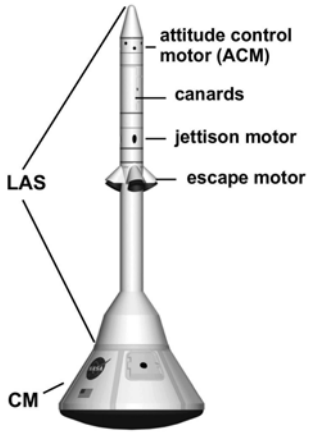

Figure 1: Launch Abort Vehicle.

In contrast, the proposed CEV design uses an active Launch Abort System (LAS) approach that would stabilize and reorient the capsule during the launch abort maneuver using an attitude control motor (ACM) in the escape tower, in addition to the use of passive canards. The use of the active system should provide a substantial weight savings by enabling elimination of the ballast that would otherwise be required to ensure passive aerodynamic stability, as well as the elimination of the open-loop pitch motor weight that was also included in the passive Apollo system. The total potential weight savings benefit for the CEV would be reduced by the weight of the ACM system and its associated propellant.

Another anticipated benefit of the active LAS approach would be improved robustness to variations in tipoff conditions at abort initiation. The ascent abort is by nature a highly dynamic maneuver, requiring safe and rapid departure from a failing booster vehicle that is potentially experiencing high angular rates and off-nominal attitudes. The use of an active system would levy some cost in the form of additional sensing, feedback, and actuation requirements, but the overall payoff could be substantial in terms of weight savings and improved safety. This paper presents an evaluation of the performance of a design for the active LAS. In this paper, the LAS will refer to the escape motor canard system, attitude control motor, and boost protective cover that compose the system designed to pull the Crew Module (CM) away from the failing CLV.

A feedback control algorithm is being developed that issues commands to the ACM system to stabilize and reorient the LAV during the abort. The controller uses a proportional/integral/derivative (PID) approach to control attitudes and rates of the LAV. The concept of operation and event sequencing during an abort varies with altitude as described in Figure 2. The LAS aborts are divided into three regimes by altitude above ground level (AGL) at abort initiation: Low - 0 to 25 kft.; Middle- 25 kft. to 150 kft.; High - 150 kft. to nominal LAS jettison. The sequence of events during an abort is based on abort initiation altitude, time elapsed from abort initiation, and on estimated dynamic pressure ($\bar{q}$) and Mach (M). For instance, at abort initiation altitudes between 7 and 25 kft., the reorientation maneuver is initiated at the elapsed time between 8 and 15 seconds at which the $\bar{q}$ estimate first drops below 100 psf. In the event that $\bar{q}$ does not go below 100 psf 15 seconds after the initiation of the abort, the controller still begins the reorientation maneuver at that time.

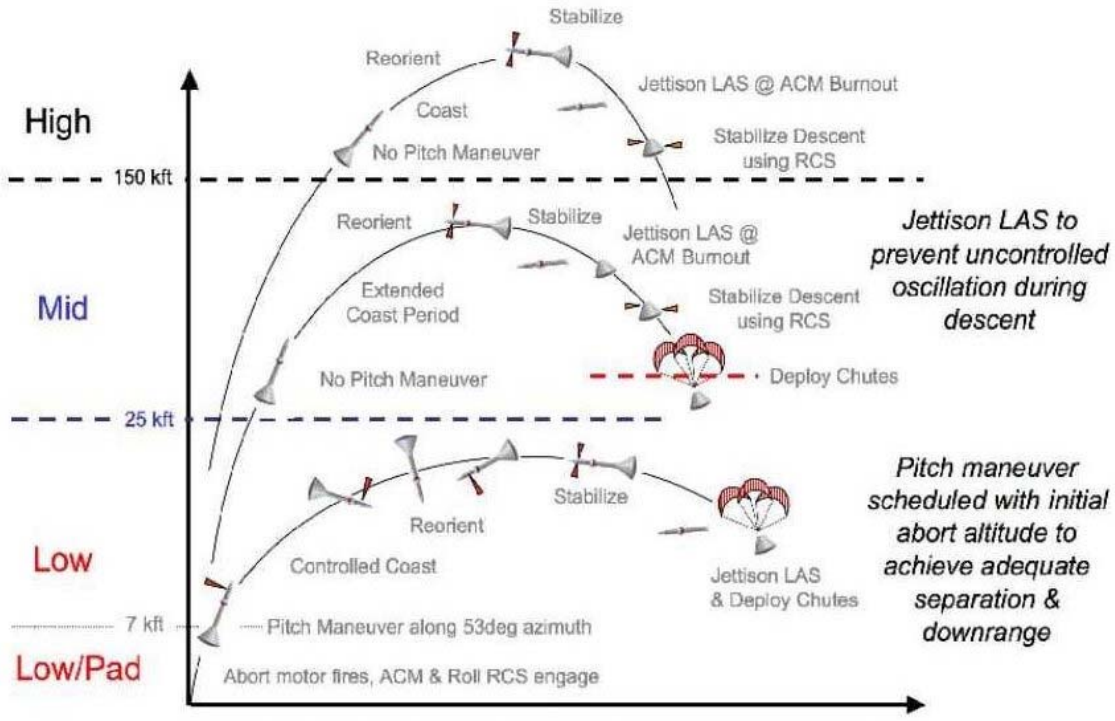

Figure 2: Concept of operation and event sequencing for active launch abort system.

II. Simulation Description

Two different simulation tools are used in the analysis of the LAS controller. In the case of the abort trajectory survey analysis, the MATLAB®/Simulink® environment is used. For the Monte Carlo analysis, all work is performed with the Advanced NASA Technology Architecture for Exploration Studies (ANTARES) Version 07.1.0 code[2]. ANTARES is a code that uses the Trick Simulation Environment[3] for defining and tying together various dynamical and environmental models, for 6-DOF simulation implementation. Only the ascent portion of the simulation is used for this study, although ANTARES contains the vehicle-specific data files (e.g., mass properties, LAS engine locations and thrust profiles, aerodynamics, etc.) as well as the model components, necessary to provide simulation capability for the ascent, on-orbit and entry phases of the CEV mission.

A. Model Description

The vehicle-specific data in these simulations is based upon the LAV aerodynamics model and mass properties for a mission to the International Space Station (ISS), carrying 3 or more crewmembers. This specific mission scenario is selected for evaluation because of the high LAV masses involved, as compared to other missions. The 1999 Global Reference Atmospheric Model[4] (GRAM-99) is used to provide the required atmospheric properties. The GRAM model also provides winds for the middle and high altitude abort simulations; however, a set of measured wind profiles for the Kennedy Space Center (KSC) launch site is substituted for low altitude (under 10 kft.) aborts. This winds data set consists of 1902 different wind profiles[5] measured at the Kennedy Space Center (KSC) launch site (wind direction and speed as a function of altitude, up to 10 kft.), taken over different months, to form a database of typical winds with seasonal variations as well as variations due to the time of day (e.g., wind changes from morning to evening over a day). The gravity model used in this study assumes an oblate (with J2 effects only), rotating Earth.

B. Monte Carlo Description

The performance of the baseline controller, under ``nominal" abort conditions (i.e., with no dispersions to the base LAV design parameters), has been evaluated and has been found to meet the performance requirements. To help test the controller under potential uncertainties and possible variations in the LAV system parameters, a series of Monte Carlo runs are executed. The perturbations in these Monte Carlo runs include the following system

parameters: 1) LAS escape motor alignment and thrust output (due to temperature variation); 2) LAS Active Control Motor and escape motor points of action; 3) aerodynamic data; and 4) LAS and CM mass properties (i.e., mass, inertia and center of mass locations). Also, variations in atmospheric properties are provided by the GRAM-99 model.

In addition to the system parameter dispersions, variations in initial flight conditions (for LAV abort initiation) are also included. These dispersion values are taken from separate Monte Carlo runs of the CLV booster simulation, with variations in the CLV model parameters. From these CLV Monte Carlo runs, flight conditions for critical abort points along the CLV trajectory (e.g., at maximum dynamic pressure ($\bar{q}$)) are obtained for use in the LAV Monte Carlo run set. Table 1 contains the range of the values for dispersed initial flight conditions for two of the abort scenarios presented in this paper, CLV maximum $\bar{q}$ and high altitude. For the case of pad aborts, the initial flight conditions are zero.

Flight Parameter	Range for Maximum CLV $\bar{q}$	Range for High Altitude
Geodetic altitude, ft.	24,386 to 55,624	273,345 to 291,369
Geodetic latitude, °	28.62 to 28.67	29.52 to 29.59
Longitude, °	279.41 to 279.47	280.37 to 280.44
Earth-relative (ER) velocity, ft./sec.	1,206.36 to 2,210.82	6,614.93 to 6,990.04
ER flight path angle, °	44.17 to 61.58	17.53 to 19.38
ER azimuth angle, °	41.27 to 48.31	41.81 to 43.30
Angle-of-attack, °	-8.39 to 4.58	-18.72 to -8.81
Sideslip angle, °	-6.09 to 4.70	-3.68 to 3.63
Bank angle, °	-179.99 to 179.89	179.99 to 179.99
Yaw body rate, °/sec.	-0.69 to 0.81	-0.05 to 0.07
Pitch body rate, °/sec	-0.61 to 1.23	-1.05 to 0.53
Roll body rate, °/sec.	-0.39 to 0.37	-0.61 to 0.49

Table 1: Initial condition variations for Monte Carlo runs.

III. Performance Evaluation Criteria

To investigate the performance of the controller, a set of criteria is developed, based upon the current functional requirements of the LAS. For a given abort simulation run to be deemed successful, the following should be met: 1) reorientation of the LAV, and staying within specific flight condition limits for successful LAS jettison and drogue parachute deployment; 2) staying under aerodynamic loading limits on the LAS during the abort maneuver to ensure structural integrity; and 3) for the specific case of aborts from the launch pad, achieving the required downrange and altitude targets for reaching the offshore distance to ensure safe water landing, and to escape damage due to potential explosions from a malfunctioning CLV. The specific flight parameters that are used to evaluate these criteria are summarized in the following paragraphs.

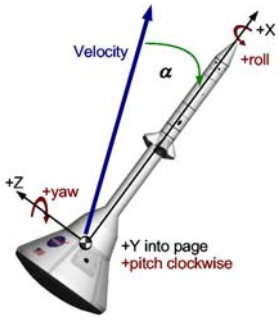

Figure 3: LAV Reference System.

The reorientation maneuver is required to change the LAV attitude to a heat-shield forward orientation. The angle-of-attack (α), as illustrated in Figure 3, is defined as 0º when the LAS is nose forward directly into the freestream, while 180º denotes the heat-shield forward orientation. To be deemed successful, the following must be true for the reorientation maneuver:

$$140° \leq \alpha_{re} \leq 220° \qquad (1)$$
$$\alpha \leq \alpha_{lim}$$

where α_{re} represents the set of α values during the last 1.5 seconds of the reorientation maneuver. The α_{lim} parameter is some maximum allowed angle-of-attack value prior to the start of the reorientation maneuver. This

latter condition is a check for any abnormally high α values, especially during the abort motor burn and the initially high ACM thrust level phase, which would be an indication of unacceptable aerodynamic loading and/or LAV tumbling during that portion of the abort trajectory.

Once the reorientation maneuver is complete, the next criteria apply to the drogue chute deployment. The time of drogue chute deployment, in relation to the end of the reorientation maneuver, is dependent on the abort altitude. However, the conditions required for successful drogue deployment are the same regardless of the abort time. The following flight conditions should be met for a successful deployment:

$$\begin{gathered} 140° \leq \alpha \leq 220° \\ -40° \leq \beta \leq 40° \\ -80°/\text{sec} \leq p \leq 80°/\text{sec} \\ -40°/\text{sec} \leq q \leq 40°/\text{sec} \\ -40°/\text{sec} \leq r \leq 40°/\text{sec} \\ 0 \leq M \leq 0.9 \\ -40 \text{ psf} \leq \bar{q} \leq 40 \text{ psf} \end{gathered} \tag{2}$$

where: β is the sideslip angle; p, q, and r are the roll, pitch and yaw body rates, respectively; M is the Mach number; and $\bar{q}$ the dynamic pressure. Due to oscillations in the body rate magnitudes, there is a very high likelihood of missing their peak values, if considered only at a single point in time. Thus, they are evaluated over a specific time interval around the point of drogue chute deployment. The maximum magnitude of the rates within that interval should meet the above tolerances for successful drogue deployment. The other parameters are evaluated at the chute deployment point.

Next, the loads induced upon the LAV during the abort are evaluated. This is done by monitoring the following parameters:

$$\begin{gathered} \bar{q} * \alpha_{total} < 17{,}000 \text{ psf*deg.} \\ \bar{q}_{can} \leq 100 \text{ psf} \end{gathered} \tag{3}$$

with $\cos(\alpha_{total}) = \cos(\alpha)\cos(\beta)$, and $\bar{q}_{can}$ represents the dynamic pressure while the canards are deployed. Exceeding the former means the destruction of the LAV, while exceeding the latter may result in damages to the canards, which are vital for reorientation.

The final set of performance criteria to be examined, exclusively for the pad abort case, involves the distance from the pad and altitude at LAS jettison. For success, the following conditions should be satisfied:

$$\begin{gathered} dpr \geq 3300 \text{ ft.} \\ \text{h} \geq 5300 \text{ ft.} \end{gathered} \tag{4}$$

where dpr is the dot product range from the launch pad to the point of LAS jettison, measured over an oblate spheroid, and h is the geodetic altitude at LAS jettison. The range and altitude target values in Eq. (4) were determined in a previous study, in which the worst-case wind profile (in terms of onshore winds possibly blowing the CM on chute back over land) from the KSC 1902 data set, was used in a separate CM chute model analysis. This chute analysis resulted in the minimum altitude and range from the pad, at the LAS jettison point, from where the CM on the chute would still land offshore in waters of at least 10-foot depth, as per current requirement, in the presence of these worst-case winds.

In addition to the above parameters, other performance metrics are also evaluated, although not to the level of pass or fail grading of controller performance results. For example, the total propellant consumption of the CM's reaction control system (RCS) and the individual RCS thruster commanded on-times; the current Concept of Operations (ConOps) relies on the CM's RCS to help provide attitude and rate control. These performance values are computed to help define RCS propellant and duty cycle requirements for the current design. Performance plots for these are included in the Monte Carlo abort simulation results discussed below.

IV. Ascent Abort Trajectory Surveys

Abort simulations are initiated at 1-second intervals along a nominal CLV ISS ascent trajectory from pad to 300 kft. altitude to confirm that the active LAS system could provide abort coverage throughout the ascent. The simulations are run with the nominal (non-dispersed) model, and with zero imparted angular rates and attitudes at abort initiation. This set of simulated aborts, called an ascent abort trajectory survey, is used to verify that the controller gains and event sequencing parameters are appropriately scheduled to provide acceptable performance in all flight regimes. This simulation does not include a chute model (though it does include Crew Module RCS), and so the runs were generally terminated shortly after LAS jettison.

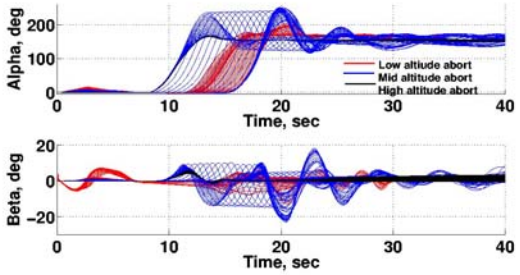

Figure 4: Angles of attack and sideslip time histories from LAS ascent aborts initiated at 1-second intervals along CLV ascent trajectory from the launch pad to 300 kft.

Time histories from the ascent abort trajectory survey are shown in Figure 4. The time histories are color-coded by altitude at abort initiation per the annotation in the figure. The top portion of the figure shows angle-of-attack plotted against time from abort initiation. The angle-of-attack variation during the first 5 seconds of the low altitude aborts indicates the initial pitch maneuver that is performed to direct the abort trajectory away from the launch pad and out over the water. The maneuver to reorient the LAV from an apex-forward to a heat-shield forward attitude can also be seen in the angle-of-attack time histories. The lower portion of the figure shows sideslip angle plotted against time from abort initiation. Again, the sideslip variations due to the initial pitch maneuver in the pad abort regime, and then the larger variations due to the reorientation maneuver, are apparent in the figure. The simulation time histories for each abort regime are examined more closely in the following section

A. Low Altitude and Pad Abort Regime

Angle-of-attack and sideslip time histories from the Low Altitude portion of the abort trajectory survey are plotted in Figure 5. The Low Altitude abort regime includes aborts initiated from the launch pad up to 25 kft. AGL. An initial pitch maneuver that directs the flight path away from the launch pad along a 53° azimuth (which is approximately normal to the coastline at the KSC launch site) is executed for aborts up to 7,000 ft. The first 5 seconds of the time histories in Figure 5 depict the angle-of-attack and sideslip variation during this maneuver. The maximum angle-of-attack is approximately 18°.

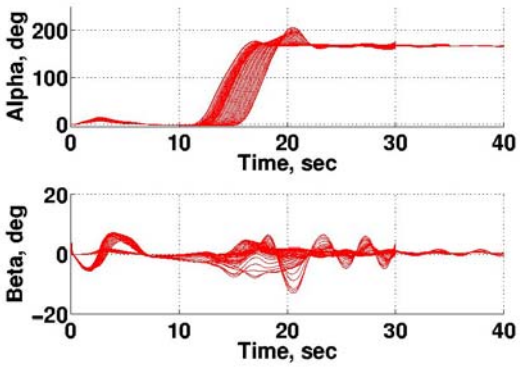

Figure 5: Angle-of-attack and sideslip time histories from the Low Altitude portion of the abort trajectory survey.

There is a downrange and altitude requirement of 3,300 ft. and 5,300 ft., respectively, that the trajectory must achieve at LAS jettison to ensure a successful chute deployment and water landing following a pad abort. To achieve these requirements, the pitch maneuver must be performed during the escape motor burn, so that the escape thrust is directed along the proper trajectory. The brevity of the escape motor firing period (approximately 4 seconds) means that the pitch maneuver must be fairly abrupt if it is to be effective in directing the abort trajectory. The high rate and large attitude change required by the pitch maneuver in the pad abort regime make it one of the most demanding of all the abort cases in terms of the authority required from the ACM. Sufficient control authority must be provided to ensure that the LAV does not tumble due to escape motor thrust misalignments or aerodynamic uncertainties during this portion of the abort.

After the pitch maneuver, a coast period at zero angle-of-attack and sideslip ensues, followed by the reorientation to a heat-shield forward attitude. In the low altitude regime, for initial altitudes less than 7,000 ft., the

reorientation maneuver is initiated when dynamic pressure drops below 70 psf. The ACM is commanded to track the desired reorientation maneuver profile. Start of the reorientation also triggers pyrotechnic deployment of the canards to a fixed open position. The deployed canards effectively destabilize the apex-forward trim condition, ensuring that the LAV cannot inadvertently tumble back into the apex forward attitude (which would preclude successful execution of the LAS jettison and chute deployment sequence). Following reorientation, the ACM is used to actively stabilize the LAV at the CM trim angle-of-attack until the LAS is jettisoned.

The LAS jettison is a timer-based event that occurs 21 seconds after abort initiation (for aborts up to 7,000 ft.). After LAS jettison, the apex cover is jettisoned and the chute deployment sequence begins. The altitude and downrange requirements are levied at LAS jettison. Figure 6a shows a plot of altitude vs. downrange from the launch pad for aborts with initial altitudes up to 3,200 ft. The initial altitude of the first (pad) abort is 375 ft. due to the height of the CLV on the launch pad. The abort trajectories follow an azimuth of 53° from the pad. The plots shown in this figure terminate at LAS jettison, and so the final altitude and downrange values indicate the success or failure with regard to the altitude and downrange requirements. Figure 6b zooms in on the critical area for the application of the downrange and altitude requirements. The first 3 trajectories fall short of the LAS jettison altitude requirement. Altitude and downrange performance for the pad abort are highly dependent on the mass model, aerodynamic model, assumed escape motor performance, and tuning of the initial pitch maneuver. These factors change significantly with each configuration update, and so the pad abort performance must be re-evaluated as the design continues to mature.

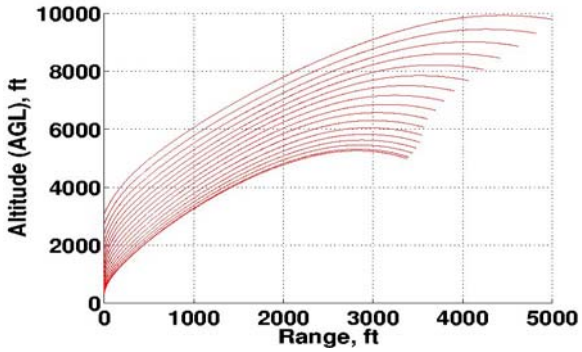

Figure 6a: Trajectories showing altitude and downrange for aborts with initial altitudes from the launch pad up to 3,200 ft.

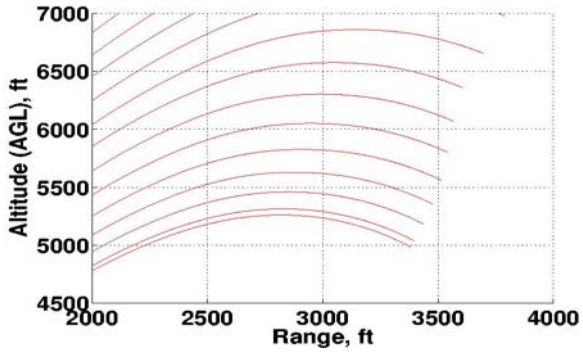

Figure 6b: Expanded excerpt of Altitude vs Downrange from Figure 6a showing failure of first 3 trajectories to meet required altitude of 5,300 ft. at LAS jettison.

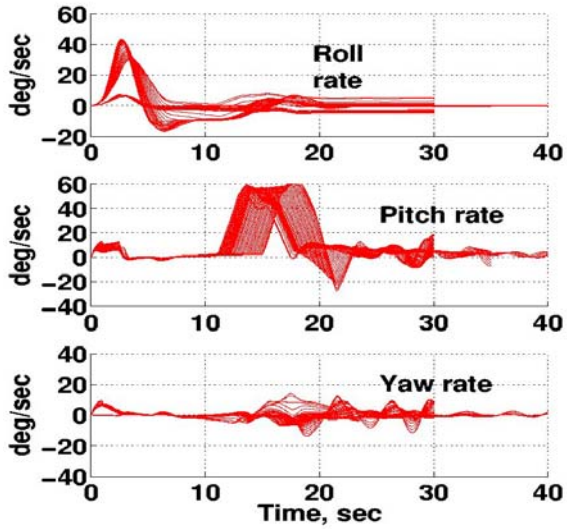

Figure 7: Time histories of body axis roll, pitch, and yaw rates for launch aborts conducted in the low altitude regime.

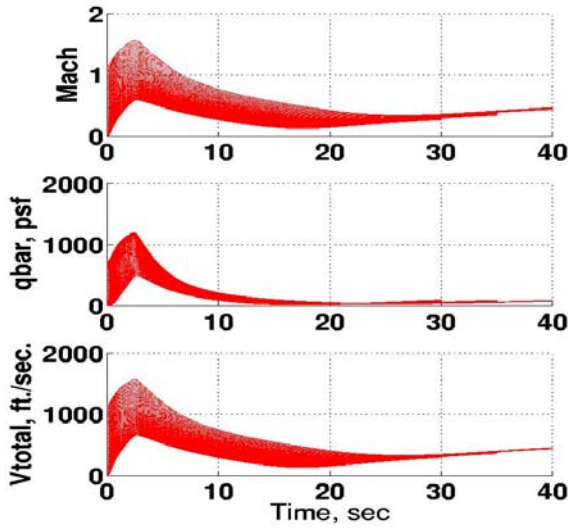

Figure 8: Time histories of Mach number, dynamic pressure, and total airspeed for aborts in the low altitude regime.

Time histories of body axis roll, pitch, and yaw rates are shown in Figure 7. The LAV configuration evaluated in this report includes the use of RCS thrusters on the CM for roll control during the abort. The pitch and yaw RCS thrusters are not used prior to LAS jettison, because the high pitch and yaw inertia values of the LAV configuration render them ineffective. These roll thrusters would operate through the LAS boost protective cover, and would be engaged at the initiation of an abort. The roll rate time histories in Figure 7 show that this is an effective approach to controlling roll disturbances that are induced during the initial pitch maneuver. The ACM is used for pitch and yaw control during the abort. The pitch rate time histories shown in Figure 7 indicate that a peak pitch rate of approximately 60°/sec. is incurred during the reorientation maneuver for aborts in the low altitude regime. Yaw rate is controlled to less than 20°/sec. The range of dynamic pressure, Mach number, and velocity relative to the atmosphere experienced during aborts conducted in the low altitude regime is shown in Figure 8; peak transonic velocities occur around 3 seconds.

B. Middle Altitude Abort Regime

The Middle Altitude abort regime includes aborts initiated from 25 kft. up to 150 kft. This regime contains the maximum dynamic pressure and maximum drag abort conditions, which drive requirements for the LAV structure and the escape motor thrust levels. Time histories of angle-of-attack and sideslip for aborts conducted in the middle altitude regime are shown in Figure 9.

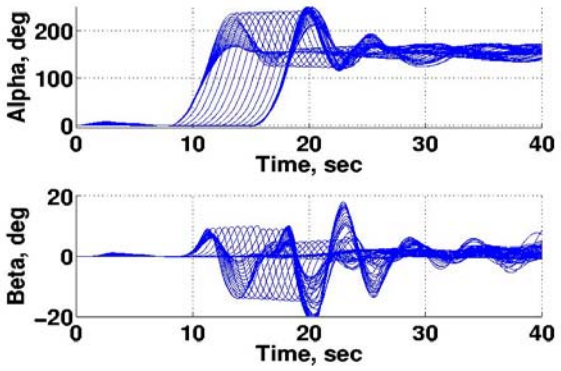

Figure 9: Angle-of-attack and sideslip time histories from the middle altitude portion of the abort trajectory survey (initial altitudes from 25,000 ft. up to 150,000 ft.).

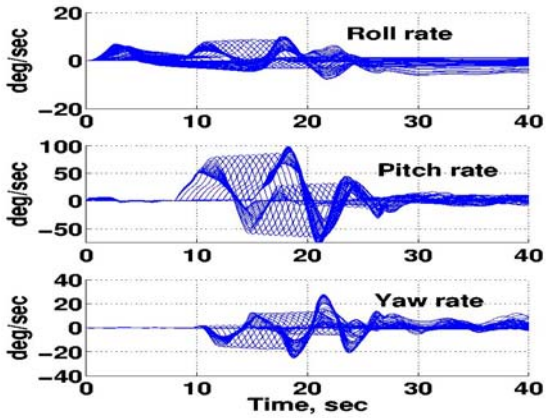

Figure 10: Time histories of body axis roll, pitch, and yaw rates for launch aborts conducted in the middle altitude regime.

The reorientation maneuver generates large amounts of overshoot for many of the lowest altitude aborts in this regime due to the high dynamic pressure at which the maneuver is initiated. The reorientation must begin no later than 15 seconds into the abort in order to stabilize in the heat-shield forward attitude before the ACM propellant is depleted. For a number of the aborts in this regime, dynamic pressure is as high as 120 psf at the start of reorientation. The larger torques that are produced as the LAV breaks out of the apex-forward attitude generate much higher pitch rates during the maneuver, resulting in more overshoot of the commanded reorientation attitude. A comparison of the angle-of-attack plots shown in Figure 9 with those in Figure 5 illustrates this difference. (The passive Apollo system actually tumbled for several cycles after canard deployment before settling into a heat-shield forward attitude during aborts at the maximum dynamic pressure flight condition.) Larger sideslip angle excursions are also apparent during the reorientation, again owing to the higher dynamic pressure.

Angular rate time histories from the middle altitude aborts are shown in Figure 10. The higher pitch rates incurred during the reorientation are apparent when comparing the plots shown in Figure 10 with those in Figure 7. Following the reorientation, the ACM is used to damp the rates in preparation for LAS jettison, which occurs at 27 sec. All cases shown in Figure 10 successfully damp the rates to less than 40°/sec. prior to LAS jettison. The CM is dynamically unstable in pitch at many of the LAS jettison flight conditions in the Middle Altitude regime, increasing the possibility that the CM could inadvertently flip back to an apex-forward attitude following LAS jettison. The CM RCS cannot be engaged until about a second after LAS jettison (this delay is the time it takes the boost protection cover to be jettisoned with the LAS and uncover the CM RCS pitch and yaw thrusters), so it is particularly important for the ACM to damp rates to the lowest levels possible prior to LAS jettison. The system performance appears acceptable for the surveys of the nominal vehicle model, but Monte Carlo variations of mass

and aerodynamic parameters (discussed later in this paper) have indicated that several cases can fail due to inadvertent reorientation of the CM immediately following LAS jettison.

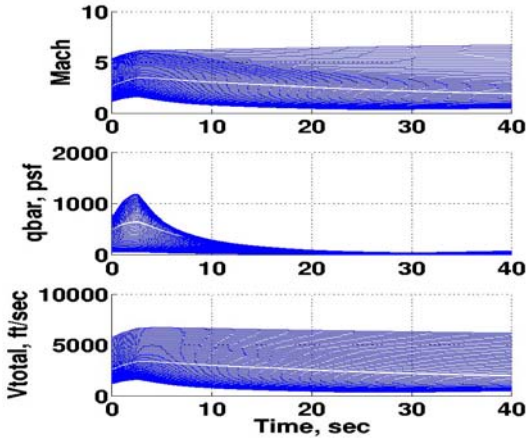

Figure 11: Time histories of Mach number, dynamic pressure, and total airspeed for aborts in the middle altitude regime.

The range of flight conditions experienced during aborts in the Middle Altitude regime is shown in Figure 11. The CM by itself exhibits a dynamic pitch instability about the heat-shield forward trim attitude at a Mach number of approximately 1.5. The higher Mach numbers and airspeeds experienced during aborts in the Mid-altitude regime are apparent when comparing Figure 11 with Figure 8.

C. High Altitude Abort Regime

The High Altitude abort regime includes aborts initiated from 150 kft. up to the nominal LAS jettison. The nominal LAS jettison will occur at an altitude of approximately 280 kft., depending upon the CLV launch trajectory. The high altitude abort surveys were run up to abort initiation altitudes of 300 kft. to ensure that the full range of possible LAS abort flight conditions were covered. Figures 12, 13, and 14 show time histories of the aerodynamic attitudes, body axis angular rates, and flight conditions that were generated for aborts conducted at 1-second intervals along the CLV ascent in the High altitude regime. Far less variation in the dynamic response of the system is observed for aborts in this regime due to the much lower dynamic pressures at which the aborts are conducted. Figure 14 shows that dynamic pressure is less than 60 psf throughout all aborts in this regime. The angle-of-attack time histories show that the reorientation maneuver starts at 8 seconds, since the dynamic pressure criteria of $\bar{q}$ less than 100 psf is already satisfied at the beginning of the reorientation time window. Positive control of rate and attitude is exhibited through the abort since the ACM control authority is sufficient to overcome all aerodynamic torques. The current concept of operation calls for the LAS to be jettisoned 12 seconds after the start of the reorientation, which places this event at 20 seconds after abort initiation. The Mach number during these aborts range between 5.5 and 8.5 owing to the rarefied atmosphere and very high flight speeds in this regime.

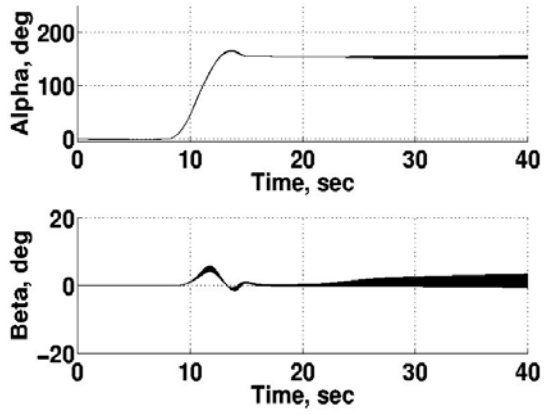

Figure 12: Angle-of-attack and sideslip time histories from the High Altitude portion of the abort trajectory survey (initial altitudes from 150 kft. up to 300 kft.).

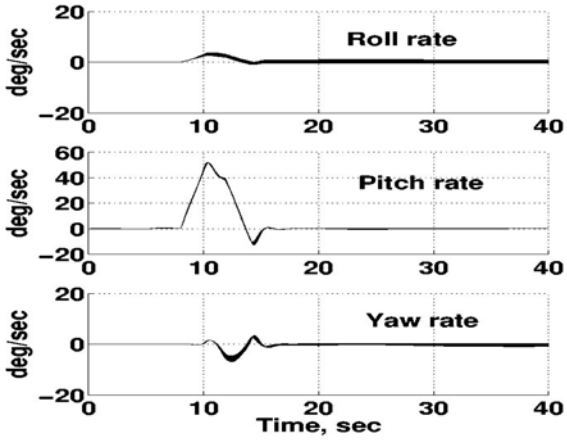

Figure 13: Time histories of body axis roll, pitch, and yaw rates for launch aborts conducted in the high altitude regime.

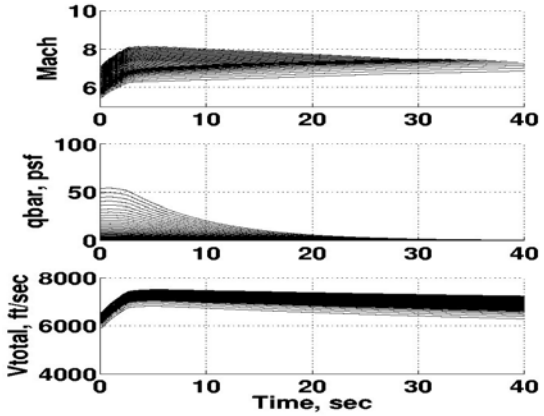

Figure 14: Time histories of Mach number, dynamic pressure, and total airspeed for aborts in the high altitude regime.

The ascent abort trajectory survey results illustrate the performance of the LAS with the nominal vehicle model in standard atmospheric conditions for aborts conducted at 1-second intervals all along a nominal CLV ascent. Several flight conditions are selected at which Monte Carlo variations of parameters associated with the propulsion model, aerodynamic model, mass model, and atmospheric conditions are examined to assess the robustness of the launch abort system design. The remainder of this paper will describe those results.

V. Monte Carlo Simulation Results

In this paper, the Monte Carlo simulation results of three specific ascent abort scenarios are presented: 1) abort at the launch pad site; 2) abort at maximum CLV $\bar{q}$; and 3) abort at high altitude (average about 280,000 ft.). For all three scenarios, the Monte Carlo simulations are executed for two variations of the ConOps: one using a single string of the RCS; and the other using two strings. Each ``string'' is comprised of 6 individual thrusters, which provide control in the following axes and directions: roll left (CRL); roll right (CRR); pitch up (CPU); pitch down (CPD); yaw left (CYL); and yaw right (CYR). The ConOps calls for the use of only a single RCS string (for system redundancy purposes), however, analysis is also continuing assuming two strings being available. All the performance figures are shown for both ConOps variations.

A. Pad Abort Scenario

For the pad abort scenario, the Monte Carlo runs consist of 1902 cases, each with one specified Kennedy wind profile and randomly selected values for the system parameters. Since this is a pad abort scenario, no variations of the initial flight conditions are defined in the Monte Carlo set. Figure 15 shows the reorientation maneuver plots. All runs meet the reorientation performance metrics defined above.

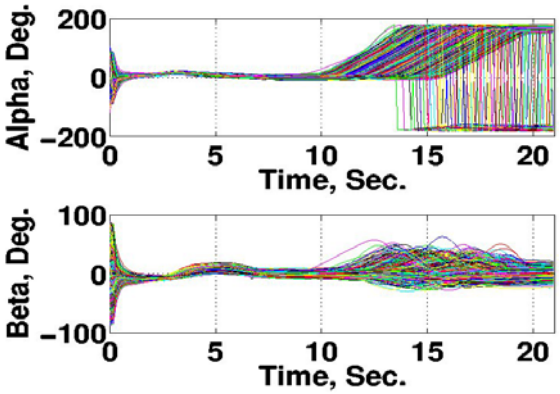

Figure 15a: Pad abort reorientation maneuver, single RCS string.

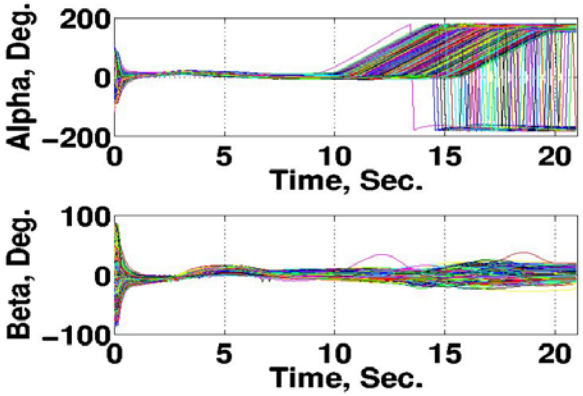

Figure 15b: Pad abort reorientation maneuver, dual RCS strings.

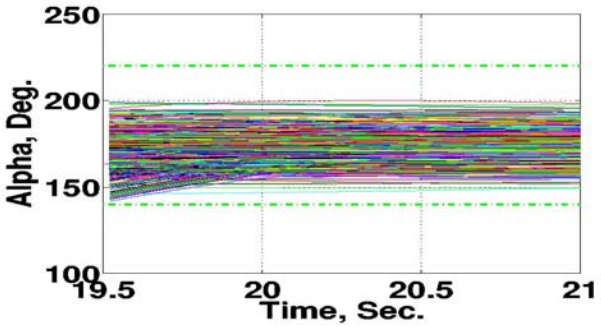

Figure 15c: Close-up of the last 1.5 seconds of the maneuver, single RCS string.

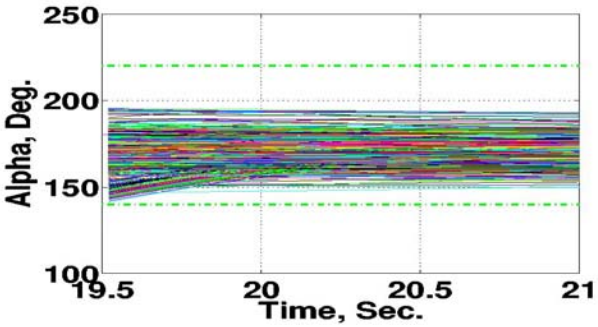

Figure 15d: Close-up of the last 1.5 seconds of the maneuver, dual RCS strings.

Figure 16 depicts the α and β value at the chute deployment point from each Monte Carlo run set. The dashed box represents the current acceptable tolerances for the two aerodynamic angle parameters. As can be seen, in both sets, all runs stay within the α-β tolerances; however, in the single string ConOps runs, several cases are closer to the lower α limit than in the two strings ConOps set. The 'x' symbols on both plots represent runs where the body rates exceed their tolerances at chute deployment. The roll, pitch and yaw body rate performances can be seen in more detail in Figure 17, Figure 18, and Figure 19, respectively. The data symbols in these rate plots are interpreted as follows: '·' indicates rates at least 10°/sec. within the rate limits; '*' are rates within 10°/sec. of the limits, but do not exceed them; and 'x' denotes those values which exceed the limits outright. Three runs exceed the rate performance limits for the single string set, while there are 4 failed runs in the dual strings set. Even though the dual strings run set has one more failure than in the single string set, it can be seen that the dual strings set has better overall rate control performance. The drogue chute $\bar{q}$ vs. M plots are shown in Figure 20. No failures are encountered in this specific metric.

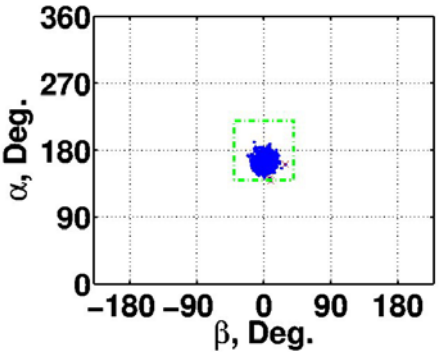

Figure 16a: Pad Abort - angle-of-attack vs. sideslip at drogue deployment, single RCS string.

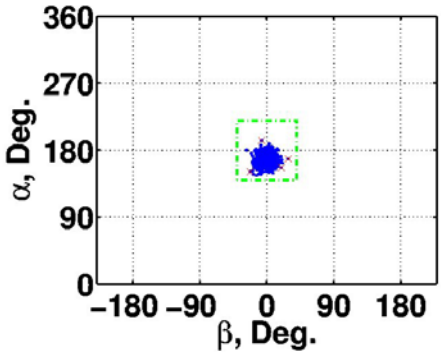

Figure 16b: Pad Abort - angle-of-attack vs. sideslip at drogue deployment, dual RCS strings.

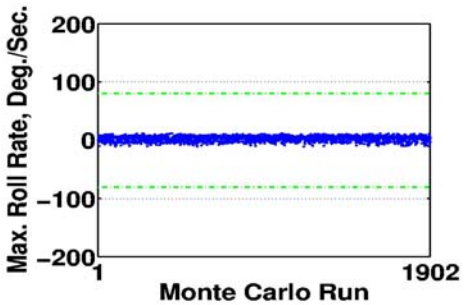

Figure 17a: Pad Abort - maximum roll rates around drogue deployment, single RCS string.

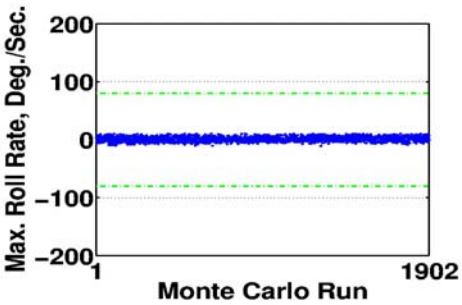

Figure 17b: Pad Abort - maximum roll rates around drogue deployment, dual RCS strings.

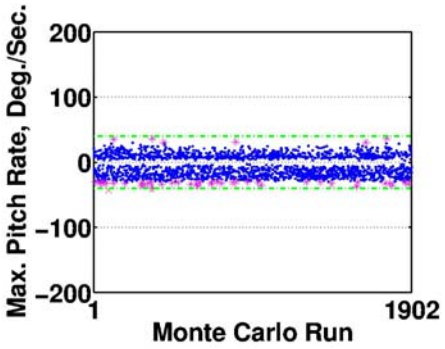

Figure 18a: Pad Abort - maximum pitch rates around drogue deployment, single RCS string.

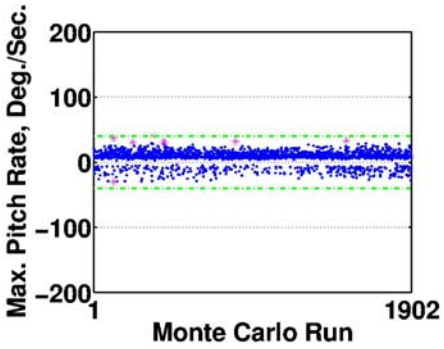

Figure 18b: Pad Abort - maximum roll rates around drogue deployment, dual RCS strings.

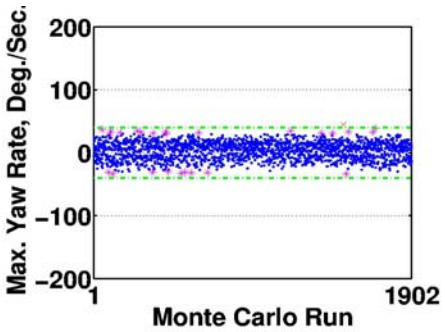

Figure 19a: Pad Abort - maximum yaw rates around drogue deployment, single RCS string.

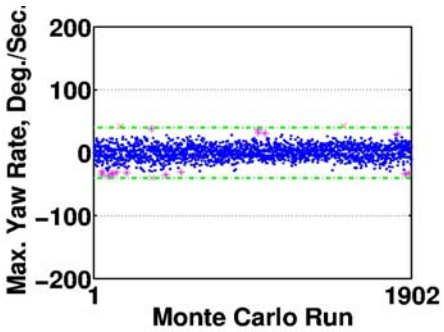

Figure 19b: Pad Abort - maximum yaw rates around drogue deployment, dual RCS strings.

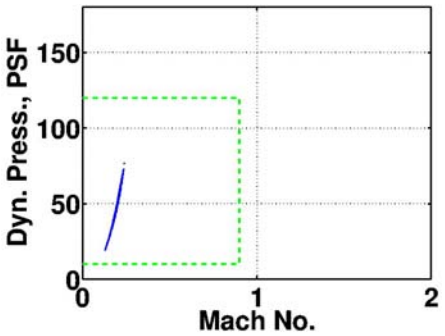

Figure 20a: Pad Abort - $\bar{q}$ vs. M at drogue deployment, single RCS string.

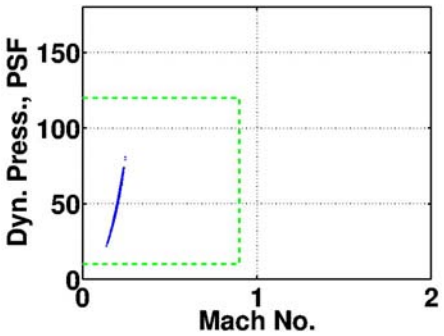

Figure 20b: Pad Abort – $\bar{q}$ vs. M at drogue deployment, dual RCS strings.

The aerodynamic loading metrics are examined. Figure 21, showing the $\bar{q} * \alpha_{total}$ time traces during the first eight seconds of the abort maneuver. The peak values occur after 3 seconds (towards the end of the escape motor burn), none of the peak values exceed the $\bar{q} * \alpha_{total}$ limit. Figure 22 plots the maximum dynamic pressure values after the canards were deployed. No runs exceed the 100-psf limit, although in several cases, that limit is approached closely.

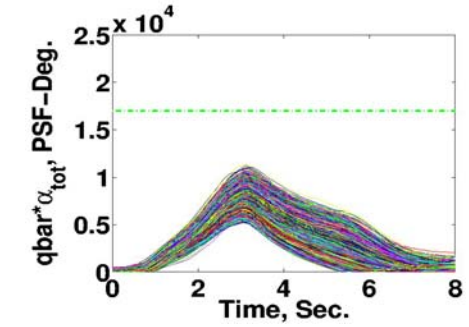

Figure 21a: Pad Abort - $\bar{q}*\alpha_{total}$, single RCS string.

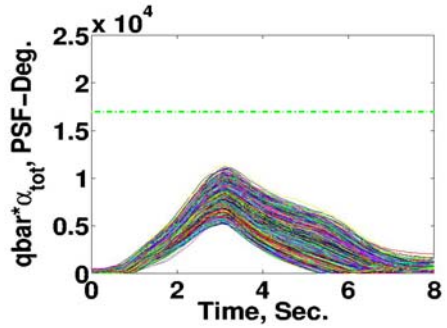

Figure 21b: Pad Abort - $\bar{q}*\alpha_{total}$ dual RCS strings.

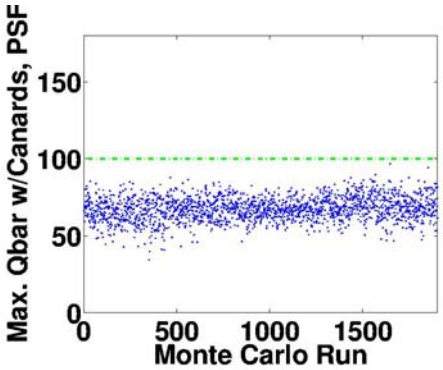

Figure 22a: Pad Abort – maximum $\bar{q}$ while canards deployed, single RCS string.

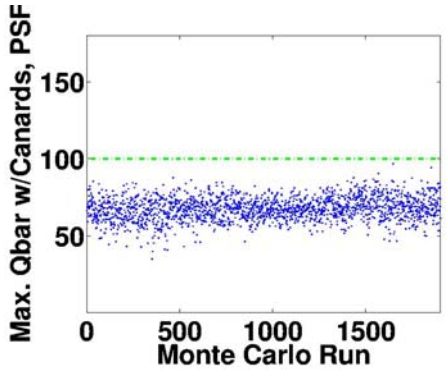

Figure 22b: Pad Abort - maximum $\bar{q}$ while canards deployed, dual RCS strings.

The results for the final performance metric, altitude and range at the LAS jettison point in the abort trajectory, is presented in Figure 23. Of the 1902 runs, 1415 cases from the single RCS string set and 1451 cases from the dual RCS strings set fail to achieve the 5300-ft. altitude target, while 201 single string cases and 196 dual strings cases fail to reach the 3300-ft. range value. Although the performance is poor for this particular metric, the abort maneuver gains within the controller can be readily adjusted to improve results.

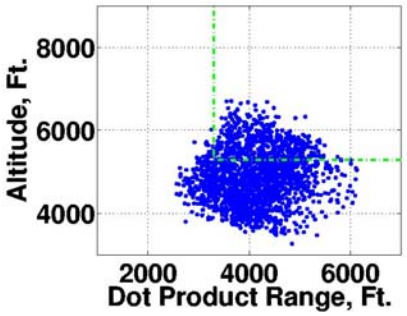

Figure 23a: Pad Abort – altitude vs. range, single RCS string.

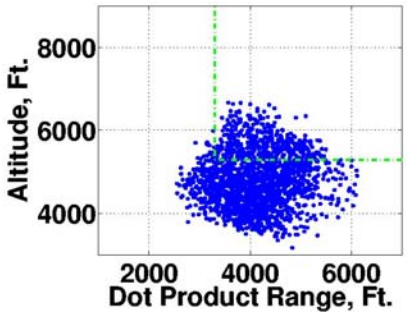

Figure 23b: Pad Abort – altitude vs. range, dual RCS strings.

Figure 24 has the total RCS propellant consumption numbers, up to the LAS jettison point. For the single string run set, the RCS fuel used ranges from 4.0 to 10.7 lb. As expected, the RCS propellant amount consumed in the dual strings set is higher, ranging from 7.2 to 16.4 lb. The RCS on-times for a RCS string, are shown in Figure 25. Although, by definition, the dual strings ConOps would have two sets of on-times, only the plots for one string out of the pair are shown, since the RCS commands from the controller are the same to each RCS string. Note that only the roll RCS is active during this portion of the abort maneuver (pre-LAS jettison). For the single string set, the roll right (CRR) and left (CRL) on-times range from 1.0 to 11.7 seconds and 3.8 to 17.3 seconds, respectively. For the

dual strings set, the roll right (CRR) and left (CRL) on-times range from 0.9 to 10.3 seconds and 2.8 to 13.8 seconds, respectively. Using two RCS strings reduces the on-times, on a per string basis.

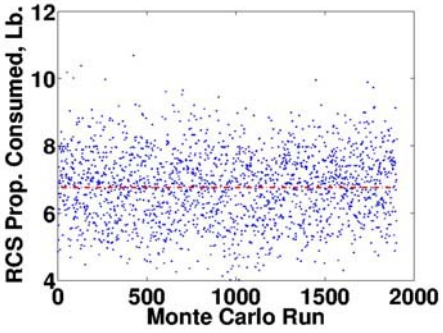

Figure 24a: Pad Abort – total RCS propellant consumption, single RCS string.

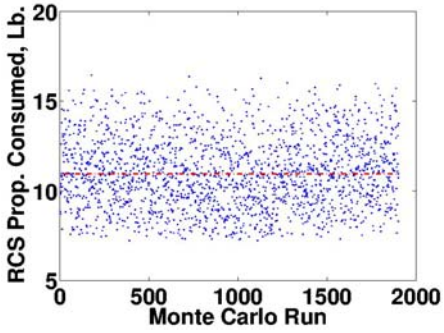

Figure 24b: Pad Abort – total RCS propellant consumption, dual RCS strings.

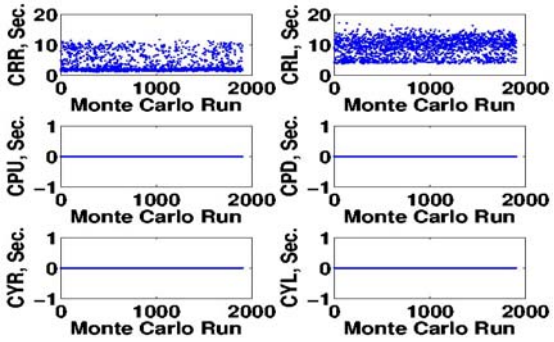

Figure 25a: Pad Abort – individual RCS thruster on-times, single RCS string.

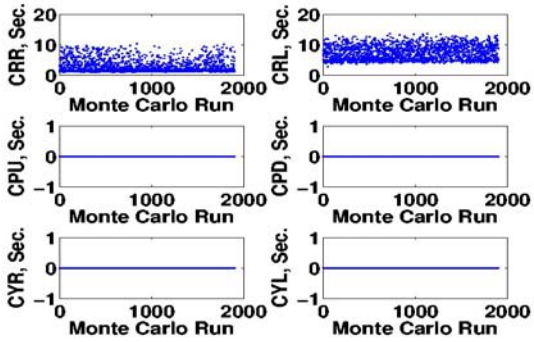

Figure 25b: Pad Abort – individual RCS on-times, dual RCS strings.

B. Maximum CLV $\overline{q}$ Abort Scenario

For the maximum $\overline{q}$ abort scenario, the Monte Carlo runs consist of 1350 cases, each with one set of specified maximum CLV $\overline{q}$ initial flight conditions and randomly selected values for the system parameters. Figure 26 shows the reorientation maneuver plots, out of the 1350 runs, 4 runs lose control and start to tumble shortly after the escape motor ignites, for both the single string and dual strings sets. For those runs which do not tumble, all single RCS string ConOps cases pass the reorientation performance metric, while only one dual strings ConOps case fails (and only by a small margin).

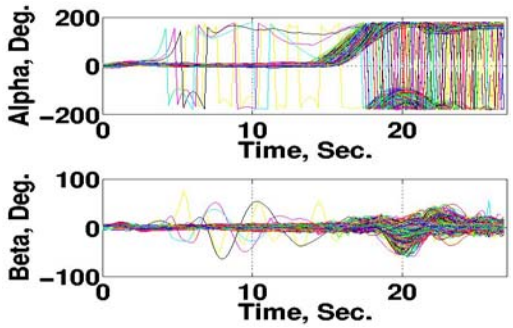

Figure 26a: Maximum CLV $\overline{q}$ Abort – reorientation maneuver, single RCS string.

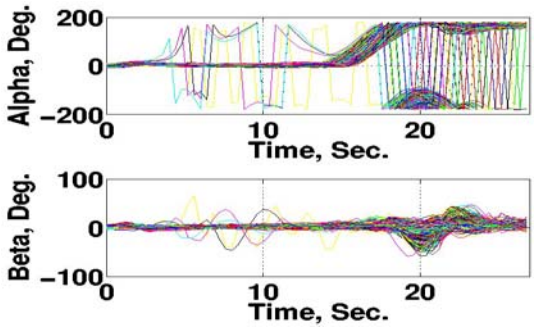

Figure 26b: Maximum CLV $\overline{q}$ Abort – reorientation maneuver, dual RCS strings.

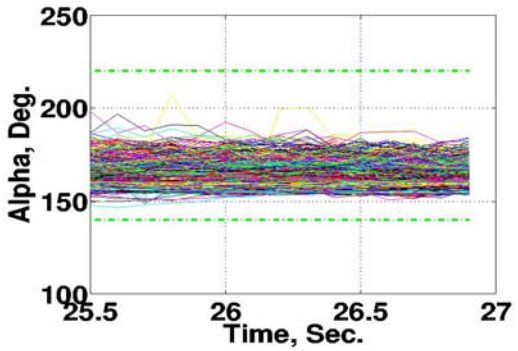

Figure 26c: Close-up of the last part of the maneuver, single RCS string.

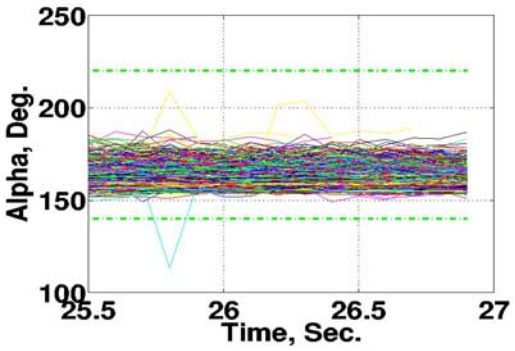

Figure 26d: Close-up of the last part of the maneuver, dual RCS strings.

Figure 27 depicts the α and β value at the chute deployment point from each Monte Carlo run set. There are 16 failures in α and 7 failures in β, for the single string set, while there are no α-β limit violations for the dual strings set. The roll, pitch and yaw body rate performances can be seen in more detail in Figure 28, Figure 29, and Figure 30, respectively. For the single string set, the numbers of failed cases are 4, 55, and 92, in roll, pitch and yaw, respectively. For the dual strings set, the numbers of failed cases are reduced to 0, 2, and 12, in roll, pitch and yaw, respectively. The rate build-up occurs as the CM must fall through the atmosphere to slow down to Mach numbers allowable for drogue deployment, as per current ConOps. The drogue chute $\bar{q}$ vs. M plots are shown in Figure 31. No failures are encountered in the M metric, however, there are 137 and 138 violations in the $\bar{q}$ limit, respectively. In those specific cases, the CM reaches relatively low altitudes before slowing down enough to be able to deploy the drogue, which result in the dynamic pressure tolerance excursions.

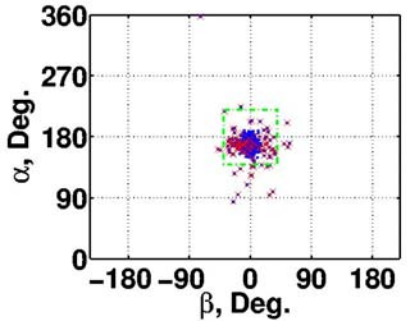

Figure 27a: Maximum CLV $\bar{q}$ Abort – angle-of-attack vs. sideslip at drogue deployment, single RCS string.

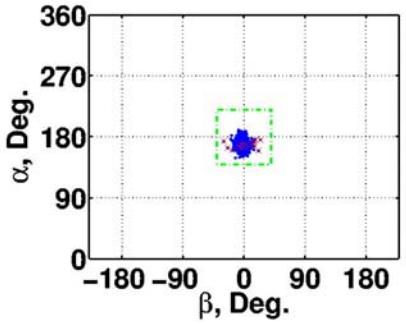

Figure 27b: Maximum CLV $\bar{q}$ Abort – angle-of-attack vs. sideslip at drogue deployment, dual RCS strings.

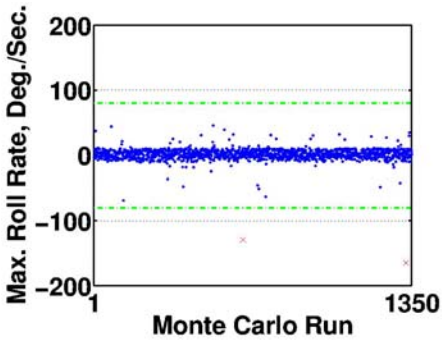

Figure 28a: Maximum CLV $\bar{q}$ Abort - maximum roll rates around drogue deployment, single RCS string.

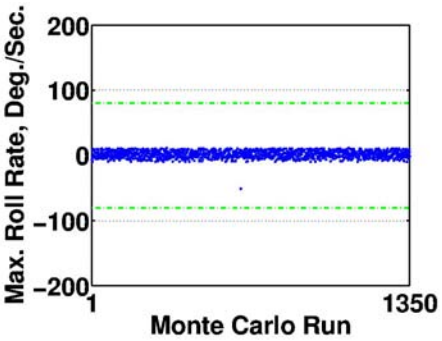

Figure 28b: Maximum CLV $\bar{q}$ Abort - maximum roll rates around drogue deployment, dual RCS strings.

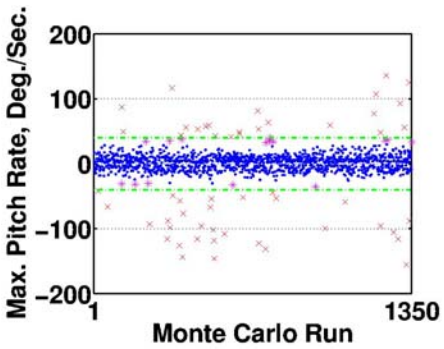

Figure 29a: Maximum CLV $\overline{q}$ Abort - maximum pitch rates around drogue deployment, single RCS string.

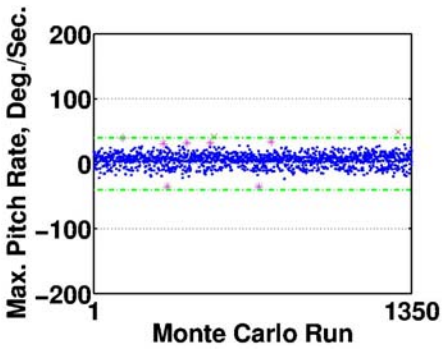

Figure 29b: Maximum CLV $\overline{q}$ Abort - maximum pitch rates around drogue deployment, dual RCS strings.

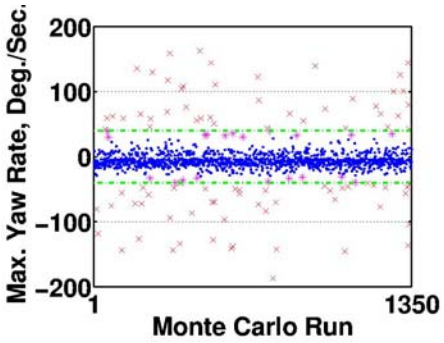

Figure 30a: Maximum CLV $\overline{q}$ Abort - maximum yaw rates around drogue deployment, single RCS string.

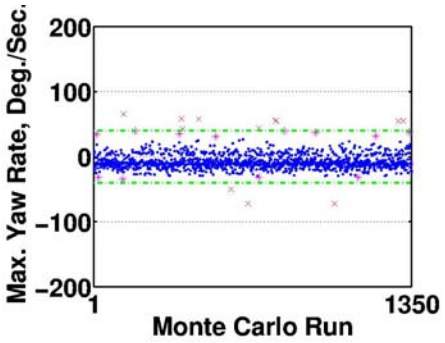

Figure 30b: Maximum CLV $\overline{q}$ Abort - maximum yaw rates around drogue deployment, dual RCS strings.

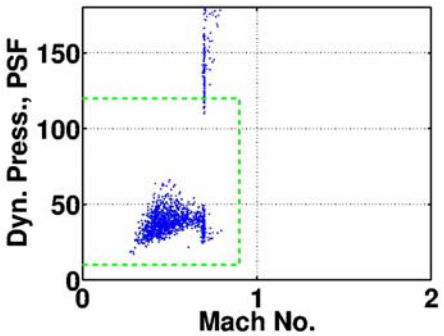

Figure 31a: Maximum CLV $\overline{q}$ Abort - $\overline{q}$ vs. M at drogue deployment, single RCS string.

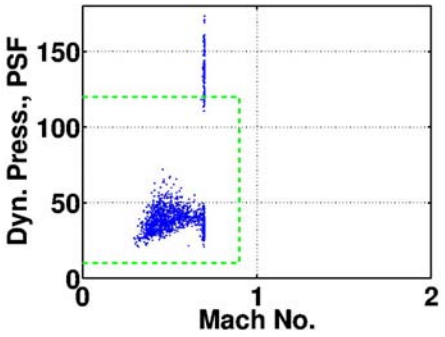

Figure 31b: Maximum CLV $\overline{q}$ Abort - $\overline{q}$ vs. M at drogue deployment, dual RCS strings.

The aerodynamic loading metrics are examined. Figure 32, showing the $\overline{q} * \alpha_{total}$ time traces during the first eight seconds of the abort maneuver. Ten out of the 1350 Monte Carlo runs, from both the single string and dual strings ConOps sets, exceed the $\overline{q} * \alpha_{total}$ limit. These include the 4 cases which tumble out-of-control, which clearly stand out. Figure 33 plots the maximum dynamic pressure values after the canards are deployed. In both run sets, there are significant numbers of cases which exceed the 100-psf limit. For the single string run set, 566 fail this metric, while 568 fail in the dual strings set. Most of these violations are not large, and there may be some reevaluation of this 100-psf value. If this limit were allowed to increase to 120 psf, these same run sets would only have 6 $\overline{q}_{can}$ limit excursions each.

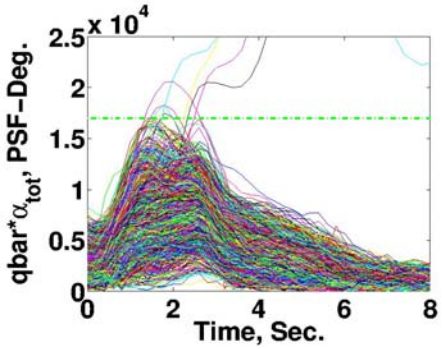

Figure 32a: Maximum CLV $\bar{q}$ Abort - $\bar{q}$ *α_{total}, single RCS string.

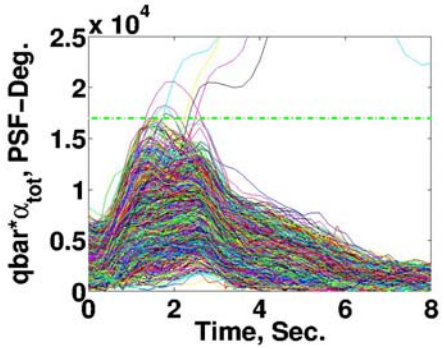

Figure 32b: Maximum CLV $\bar{q}$ Abort - $\bar{q}$ *α_{total}, dual RCS strings.

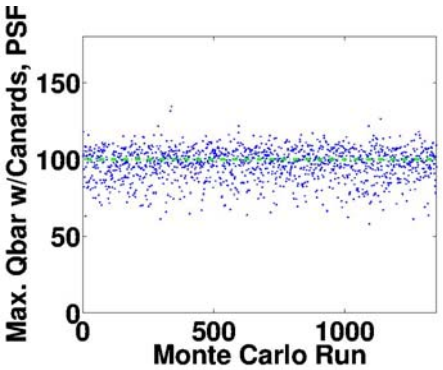

Figure 33a: Maximum CLV $\bar{q}$ Abort - maximum $\bar{q}$ while canards deployed, single RCS string.

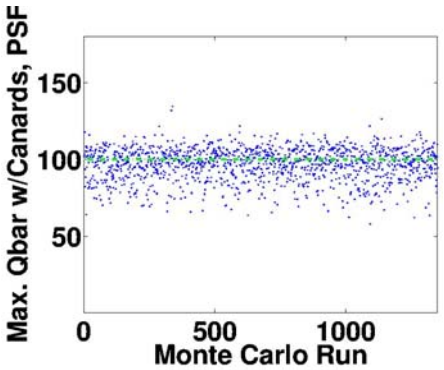

Figure 33b: Maximum CLV $\bar{q}$ Abort - maximum $\bar{q}$ while canards deployed, dual RCS strings.

Figure 34 has the total RCS propellant consumption numbers, computed up to point of drogue deployment. The current ConOps calls for the use of roll RCS thrusters only, prior to LAS jettison, then switching over to full 3-axis RCS control shortly after LAS jettison. For the single string run set, the RCS fuel used ranges from 0.6 to 45.3 lb. The RCS propellant amount consumed in the dual strings set is slightly higher, ranging from 0.9 to 48.4 lb. The RCS on-times for each RCS string are shown in Figure 35. Table 2 contains the RCS on-times for the two run sets. Using two RCS strings reduces the on-times, on a per string basis

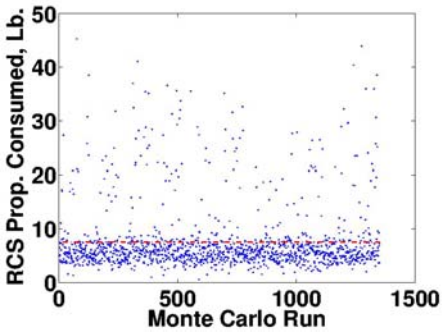

Figure 34a: Maximum CLV $\bar{q}$ Abort – total RCS propellant consumption, single RCS string.

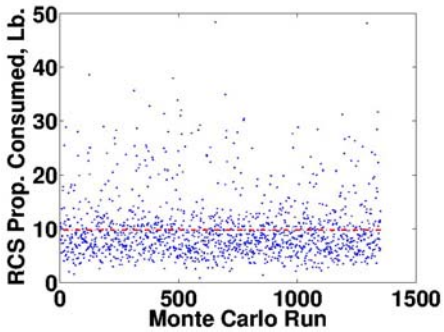

Figure 34b: Maximum CLV $\bar{q}$ Abort – total RCS propellant consumption, dual RCS strings.

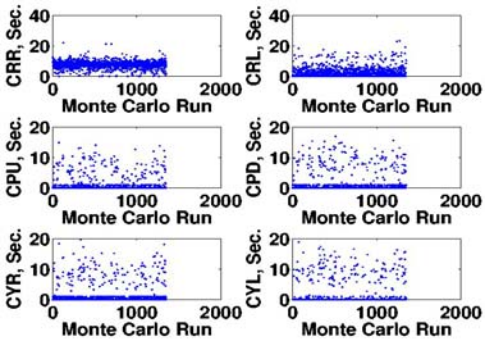

Figure 35a: Maximum CLV $\overline{q}$ Abort – individual RCS thruster on-times, single RCS string.

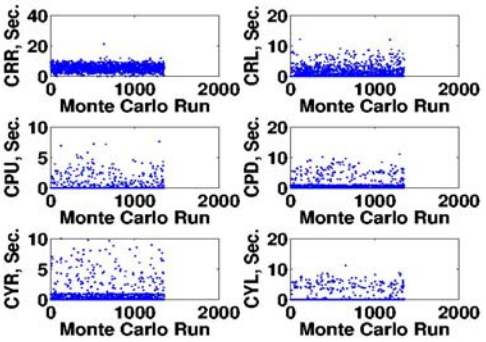

Figure 35b: Maximum CLV $\overline{q}$ Abort – individual RCS thruster on-times, dual RCS strings.

RCS Thruster	Single String On-Times, sec.	Dual Strings On-Times, sec.
Roll right	0.0 to 22.12	0.0 to 21.24
Roll left	0.0 to 23.32	0.0 to 12.16
Pitch up	0.0 to 14.88	0.0 to 7.60
Pitch down	0.0 to 16.92	0.0 to 11.08
Yaw right	0.0 to 19.60	0.0 to 10.00
Yaw left	0.0 to 18.84	0.0 to 11.08

Table 2: Range of RCS on-times for Maximum CLV $\overline{q}$ Aborts.

C. High Altitude Abort Scenario

For this high altitude abort scenario, the Monte Carlo runs consist of 1349 cases, each with one set of specified high altitude initial flight conditions (from Table 1.) and randomly selected values for the system parameters. Figure 36 shows the reorientation maneuver plots, with no failures from either RCS ConOps run set.

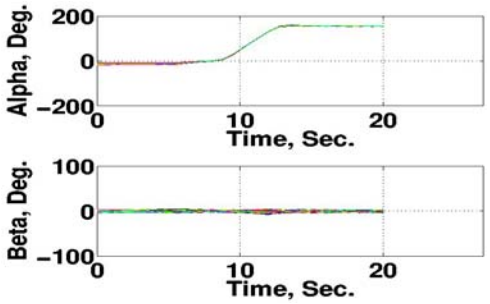

Figure 36a: High altitude abort – reorientation maneuver, single RCS string.

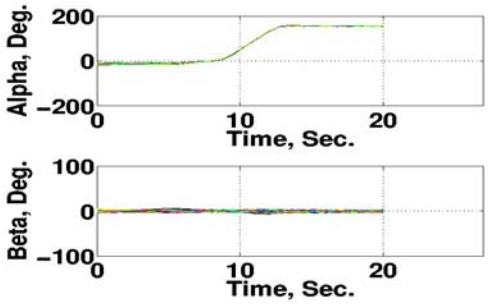

Figure 36b: High altitude abort – reorientation maneuver, dual RCS strings.

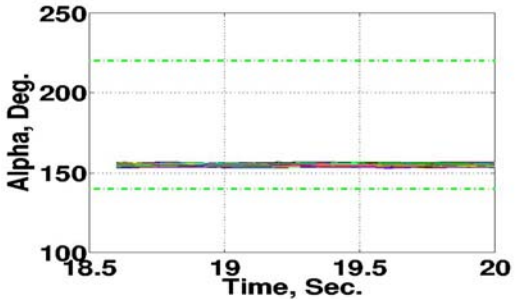

Figure 36c: Close-up of the last 1.5 seconds of the maneuver, single RCS string.

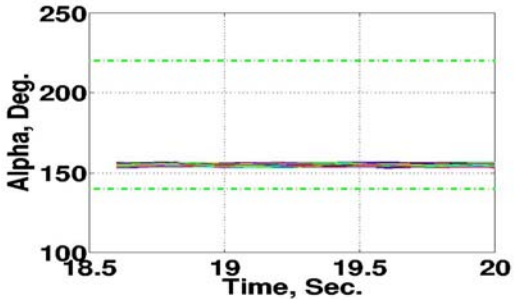

Figure 36d: Close-up of the last 1.5 seconds of the maneuver, dual RCS strings.

Figure 37 depicts the α and β value at the chute deployment point from each Monte Carlo run set. There are 107 failures in α and 97 failures in β, for the single string set, while there are 3 α limit violations and 1 in β for the dual strings set. The roll, pitch and yaw body rate performances can be seen in more detail in Figure 38, Figure 39, and Figure 40, respectively. For the single string set, the numbers of failed cases are 63, 378, and 657, in roll, pitch and yaw, respectively. For the dual strings set, the numbers of failed cases are reduced to 0, 8, and 30, in roll, pitch and yaw, respectively. As in the maximum $\bar{q}$ abort scenario, the rate build-up occurs as the CM must fall through the atmosphere to slow down to Mach numbers allowable for drogue deployment, as per current ConOps. The drogue chute $\bar{q}$ vs. *M* plots are shown in Figure 41. No failures are encountered in the *M* metric, however, there are 1171 and 1141 violations in the $\bar{q}$ limit, respectively. In those specific cases, the CM reaches relatively low altitudes before slowing down enough to be able to deploy the drogue, which results in the dynamic pressure tolerance excursions.

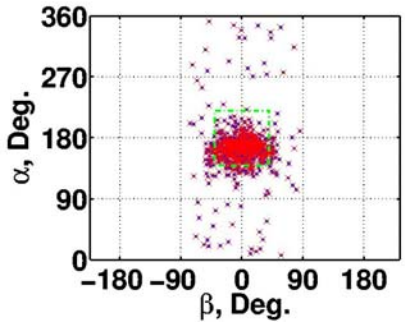

Figure 37a: High Altitude Abort – angle-of-attack vs. sideslip at drogue deployment, single RCS string.

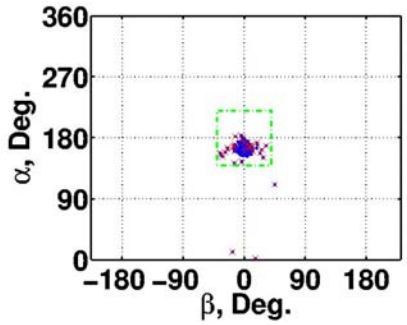

Figure 37b: High Altitude Abort – angle-of-attack vs. sideslip at drogue deployment, dual RCS strings.

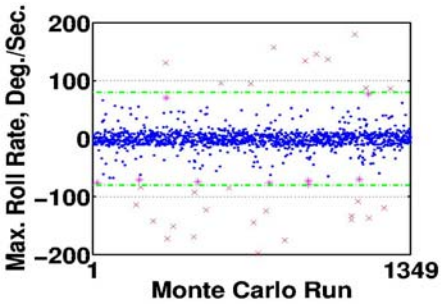

Figure 38a: High Altitude Abort – maximum roll rate around drogue deployment, single RCS string.

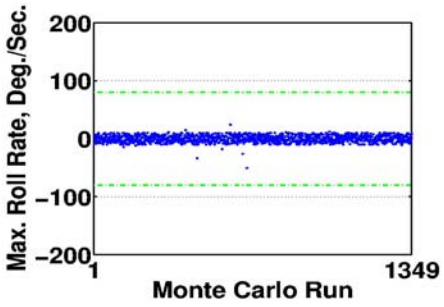

Figure 38b: High Altitude Abort – maximum roll rate around drogue deployment, dual RCS strings.

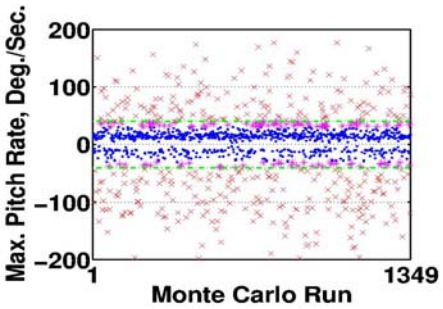

Figure 39a: High Altitude Abort – maximum pitch rate around drogue deployment, single RCS string.

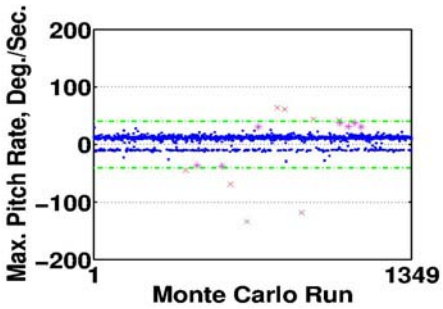

Figure 39b: High Altitude Abort – maximum pitch rate around drogue deployment, dual RCS strings.

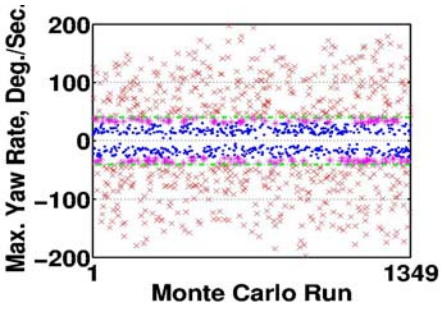

Figure 40a: High Altitude Abort – maximum yaw rate around drogue deployment, single RCS string.

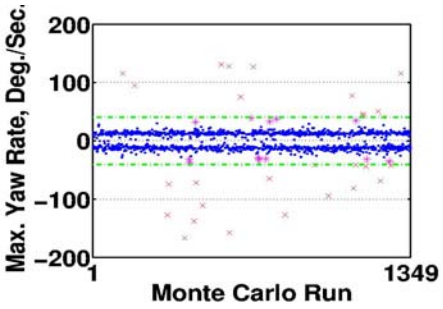

Figure 40b: High Altitude Abort – maximum yaw rate around drogue deployment, dual RCS strings.

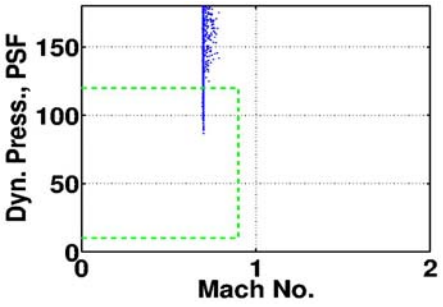

Figure 41a: High Altitude Abort – $\overline{q}$ vs. M at drogue deployment, single RCS string.

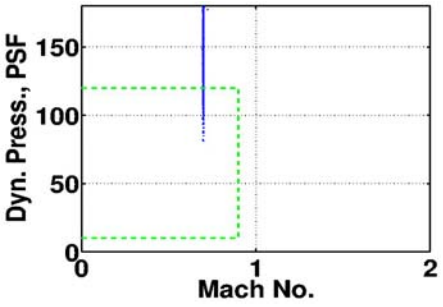

Figure 41b: High Altitude Abort – $\overline{q}$ vs. M at drogue deployment, dual RCS strings.

The aerodynamic loading metric results are shown in Figure 42 and Figure 43. Due to the high altitudes, the aerodynamic loading is not an issue for this abort scenario.

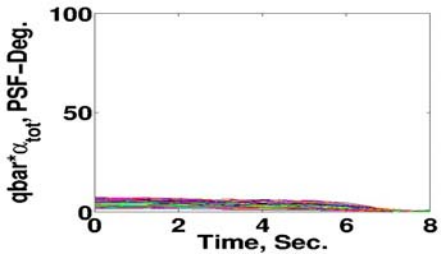

Figure 42a: High Altitude Abort – $\overline{q}$ *α_{total}, single RCS string.

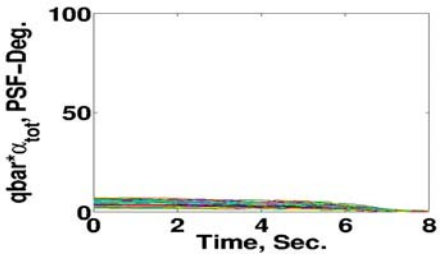

Figure 42b: High Altitude Abort – $\overline{q}$ *α_{total}, dual RCS strings.

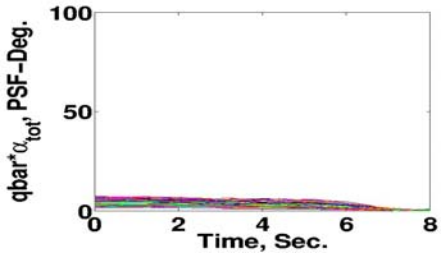

Figure 43a: High Altitude Abort - maximum $\overline{q}$ while canards deployed, single RCS string.

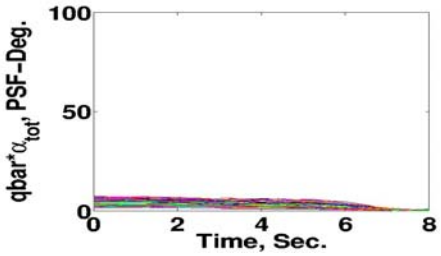

Figure 43b: High Altitude Abort – maximum $\overline{q}$ while canards deployed, dual RCS strings.

Figure 44 has the total RCS propellant consumption numbers, computed up to point of drogue deployment. For the single string run set, the RCS fuel used ranges from 0.6 to 52.2 lb. The RCS propellant amount consumed in the dual strings set is higher, ranging from 0.3 to 92.7 lb. The RCS on-times for a RCS string are shown in Figure 45. Table 3 contains the RCS on-times for the two run sets. As in the previous two abort scenarios, using two RCS strings reduces the on-times, on a per string basis

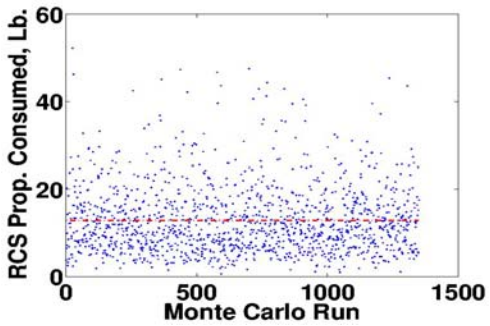

Figure 44a: High Altitude Abort – total RCS propellant consumption, single RCS string.

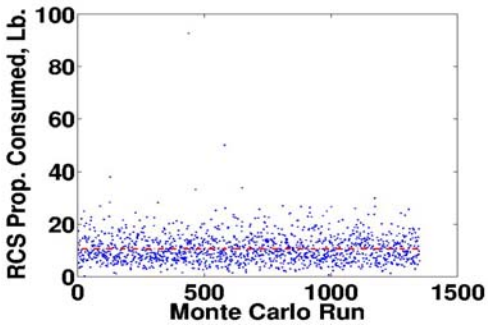

Figure 44b: High Altitude Abort – total RCS propellant consumption, dual RCS strings.

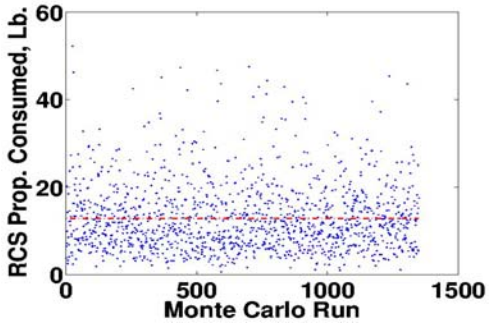

Figure 45a: High Altitude Abort – individual RCS thruster on-times, single RCS string.

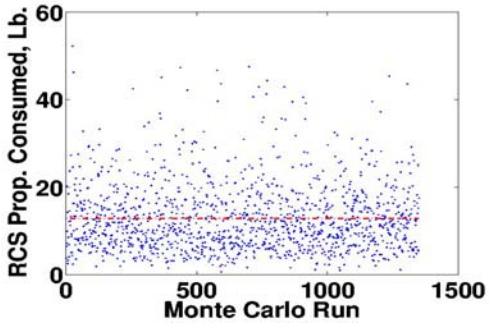

Figure 45b: High Altitude Abort – individual RCS thruster on-times, dual RCS strings.

RCS Thruster	Single String On-Times, sec.	Dual Strings On-Times, sec.
Roll right	0.0 to 19.96	0.0 to 10.44
Roll left	0.0 to 21.32	0.0 to 3.36
Pitch up	0.0 to 22.56	0.0 to 27.08
Pitch down	0.0 to 21.72	0.0 to 19.80
Yaw right	0.0 to 25.72	0.0 to 14.32
Yaw left	0.0 to 25.48	0.0 to 14.12

Table 3: Range of RCS on-times for High Altitude Aborts.

VI. Conclusions

The baseline LAV controller has been tested with the Government simulation tool, ANTARES, to evaluate the controller's capability to meet the current LAV abort performance requirements, from launch on a typical mission to the ISS. A set of pass/fail criteria was used to evaluate the controller abort performance. Three critical abort scenarios were studied: abort from the pad; abort from the maximum CLV dynamic pressure point; and abort from

high altitude. For each scenario, Monte Carlo simulation runs, with dispersions in LAV system parameters, together with variations in initial abort flight conditions, were executed to better gage the controller's performance. These Monte Carlo simulations were made for two different Concepts of Operations: 1) using only a single string of the CM's RCS thrusters; and 2) using two strings.

Overall, the performance of the controller satisfied most of the evaluation criteria. The exceptions were: the pad abort altitude/range performance; the maximum CLV $\bar{q}$ abort dynamic pressure canards-deployed limit excursions; and the drogue chute deployment dynamic pressure limit violations for both the maximum CLV $\bar{q}$ and high altitude abort scenarios. It is believed that adjustments to the controller and the Concepts of Operations specifically regarding the drogue chute deployment will eliminate most of these failures. The use of dual strings of the CM's RCS thrusters reduced the number of body rate failures around drogue deployment significantly, as seen in the maximum CLV $\bar{q}$ and high altitude abort scenarios. However, there was a corresponding jump in the total RCS propellant amount required.

References

[1]McCarthy, J. F. JR., Dodds, J. Ian, Crowders, R. S., "Development of the Apollo Launch Escape System", *J. Spacecraft*, Vol. 5, No. 8, p.927, North American Rockwell Corporation, Downey, CA, Aug. 1968.

[2]*Users Guide for the ANTARES Simulation*, Engineering Directorate, Aerosciences and Flight Mechanics Division, Johnson Space Center, Mar., 2007.

[3]Vetter, Keith, *The Trick Design Document - Trick 2004.0 Release*, Titan Corporation, Aug. 2004.

[4]Justus, C. G., Johnson, D. L., "The NASA/MSFC Global Reference Atmospheric Model - 1999 Version (GRAM-99)", NASA-TM-1999-209630, May 1999.

[5]Brown, S. C., "150 Per Month Jimsphere Wind Speed Profiles for Aerospace Vehicle Design Capability Studies, Location: Kennedy Space Center", MSFC-ES81, Feb., 1978.